

SUBSIDENCE MEASUREMENT WITH PS-INSAR TECHNIQUES IN SHANGHAI URBAN

Lijun Lu Mingsheng Liao

State Key Laboratory for Information Engineering in Survey, Mapping and Remote Sensing, Wuhan University Luoyu Road 129, Wuhan, P.R. China, 430079, lulijun@lmars.whu.edu.cn

Commission VII, WG VII/2

KEY WORDS: DInSAR, PS-InSAR, Subsidence, Measurement, Urban

ABSTRACT:

Spaceborne SAR Differential interferometry (DInSAR) has been used to monitor some geological disasters such as ground subsidence. This paper applies two Permanent Scatterer InSAR (PS-InSAR) techniques to measure long-term and short-term subsidence in urban area of Shanghai urban. A great number of archived ERS data are utilized to measure long-term subsidence during 1993-2000 year. A small set of ASAR data are utilized to measure short-term subsidence during 2003-2005 year. The subsidence measurement results are examined with simultaneous leveling during the two periods, and comparison result shows a good agreement. Furthermore, the causes of subsidence are qualitatively analyzed in the main subsidence regions of Shanghai urban, and the variation of subsidence in two different periods can be detected according to the obtained subsidence measurement results.

1. INTRODUCTION

The surface deformations monitoring using DInSAR technique has shown some good results in the last years of research. As the extension of DInSAR technique, PS-InSAR technique has been recognized as a powerful tool for large-scale and long-term monitoring small surface deformations in urban areas (Li, Liao et al., 2004). The strategies of PS technique is to find point-wise permanent scatters (hereafter called PSs) that exhibit phase stability over a long period of time, estimate and remove atmospheric phase contribution, DEM error and system/thermal noise etc., and finally measure precise displacement on permanent scatters. The advantage of PS-InSAR technique lies in that it can practically overcome the problems of geometrical and temporal decorrelation existing in DInSAR by using a large amount of SAR data.

In this paper, PS-InSAR techniques are applied to the subsidence measurement in Shanghai urban as Shanghai urban has been suffering the subsidence disaster since 1920s. Aiming to the different survey applications, this author utilized the two PS-InSAR techniques on two different amount of SAR dataset. In the first study, the long-term subsidence can be measured by applying traditional PS-InSAR technique—Permanent Scatterer (Ferretti et al., 2000; 2001), as an amount of ERS-1/2 archived images from 1993 to 2000 in Shanghai urban are available from ESA. In the second study, the short-term subsidence from 2003 to 2005 in Shanghai urban can be measured. As the extension of ERS-1/2 satellite, ENVISAT satellite has just in operation for several years, only small ASAR dataset are acquired so that it is insufficient to make an analysis in long time series. Considering limitation in the data availability, another PS-InSAR technique—Spatio-Temporal Unwrapping Network (STUN) (Bert M. Kampers, 2006) can be applied. The STUN technique is improved in this paper for subsidence measurement in small dataset.

Since Shanghai government has been made continuous leveling since 1990s, it provides us a good validation standard for precise evaluation of subsidence results by two PS-InSAR

techniques. The subsidence results are validated by comparing the corresponding PSs and Leveling Benchmarks (LBs). On the basis of results validation, the causes of subsidence are qualitatively analyzed in the main subsidence regions of Shanghai urban, and the variation of subsidence in two different periods also can be detected according to the achieved subsidence results.

2. DESCRIPTION OF TEST AREA AND DATA SET

2.1 Test area

Shanghai is the largest industrial city in China, standing on the East China Sea and situated at the front edge of Yangtze Delta, as showed in the left pictures of figure.1. Subsidence due to underground water over-pumped has become a major problem in the city since 1920s. In the recent decade, with the increasing land use for urban development, the subsidence disaster has become worse. The severe subsidence generally occurred in the urban areas of Shanghai where the sites of underground water extraction and major municipal engineering constructions are located. Therefore we lay emphasis study on the urban of Shanghai, as shown by the right picture in figure.1.



Figure.1 The location of Shanghai city. The left picture shows the location of Shanghai city in China, the right picture shows the location of test area, i.e. urban of Shanghai, covering an area about 1000 km².

2.2 Data set

The 26 scenes archived complex (SLC) images (Track:3,Frame: 2979) are chosen as the long-term experimental data acquired by C-band ERS-1/2 sensors covering the time span from 1993 to 2000 in the test area. Due to enough dataset, a unique image is selected as the master image to generate temporal interferograms. The interferometric combinations ensure the uniform temporal and spatial baseline distribution, as shown in figure.2.

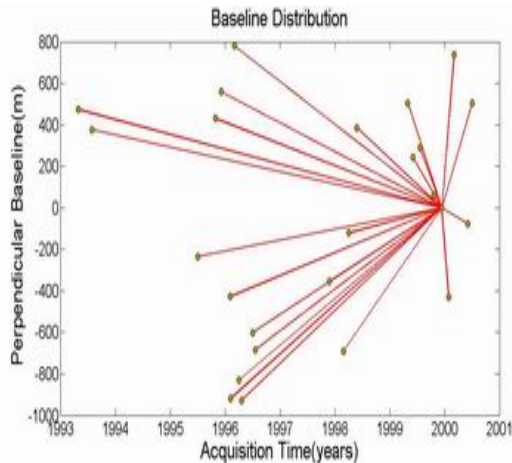


Figure 2. Interferometric combinations in long time series

The latest 9 scenes of complex (SLC) images (Track:3,Frame: 2979) acquired by C-band ASAR sensors onboard the Envisat covering the time span from 2003 to 2005 in the test area are chosen as the short-term experimental data. In order to exploit sufficient interferograms, multiple master images are chose to generate multiple interferometric combinations in overlapping time intervals with the uniform temporal and spatial baseline distribution, as shown in figure.3.

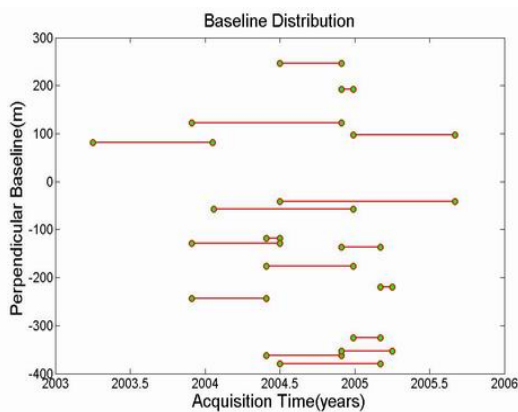


Figure 3. Interferometric combinations in short time series

Shuttle Radar Topography Mission (SRTM) DEM of low resolution of $90m \times 90m$ is used as the external DEM to remove the topography phase. The DEM is enough for our study because the test area is a flat area with maximum topographic relief less than 30m.

3. INTERFEROMETRIC PHASE MODEL

The two PS-InSAR techniques are both model-based, firstly the interferometric phase model can be expressed as the sum of the following four contributions,

$$\phi_{int} = \phi_{topo} + \phi_{defo} + \alpha_{atmos} + n_{noise} \quad (1)$$

Where ϕ_{topo} = the phase caused by topography

ϕ_{defo} = the phase caused by a displacement of the target along the line of sight (LOS) of sensor

α_{atmos} = the phase caused by atmospheric artefacts and imprecise orbit data.

n_{noise} = the phase caused by decorrelation noise.

By removing the topography phase, the differential interferometric phase model can be obtained in the Equation.2.

$$\phi_{diff} = \phi_{defo} + \phi_{topo-error} + \alpha_{atmos} + n_{noise} \quad (2)$$

Where $\phi_{topo-error}$ is the phase caused by topography error. It is expressed as Equation.3

$$\phi_{topo-error} = \frac{4\pi}{\lambda} \cdot \frac{B_{\perp}}{R \cdot \sin \theta} \varepsilon \quad (3)$$

Where λ = radar wavelength

R = range distance from master sensor to ground

B_{\perp} = the local perpendicular baseline

θ = the local incidence angle

ε = the DEM error

As the ground deformation in urban is a low velocity process, a linear model can basically fit the deformation change. So ϕ_{defo} is explicitly written as Equation.4.

$$\phi_{defo} = \frac{4\pi}{\lambda} \cdot v T \quad (4)$$

Where v is the deformation velocity in the LOS direction (subsidence velocity is approximately equal to vertical component of v), and T is the temporal baseline between two SAR acquisitions

The two PS-InSAR techniques are primitively based on the interferometric phase model represented by Equation.1.

4. PS TECHNIQUE

In the processing system of PS technique, the PSs are initially identified by means of amplitude dispersion threshold method (Ferretti et al., 2000), which is usually an effective detection method in a large amount of dataset. Based on the interferometric model, spectral estimation strategy is utilized to estimate the valid phase terms (e.g. subsidence velocity) on PSs in time series. And disturbing phase terms (e.g. atmospheric

artifacts) are compensated for at PSs by exploiting their different spectral behaviors in a multidimensional framework of time, space and normal baseline (i.e., acquisition geometry).

4.1 Processing Result

The 26 scenes of archived ERS-1/2 SLC images are processed by TRE (In the framework of Dragon I Project). 22,139 PSs are identified in the test area of about 1,000km², i.e. with a density of 22 points/ km². The subsidence velocities on the PSs from 1993 to 2000 are derived to produce the subsidence map, as showed in figure.4.

4.2 Validation

In the test area, 126 LBs were measured from 1993 to 2000 year, as showed in figure.5. The levelling campaign was made each year in this period, LBs rank Level 1, Level 2 as the levelling standards of China, with standard deviation less than 2mm. The average of multiple surveys at each LB is used as the criterion to validate the result in long time series.

Nearest neighboring method is used to validate PSs computed by PS. The distance between PSs and LBs is limited to range of 100m. Within the distance, PS closest to LP will be selected for comparison. In figure.8, 115 pairs of PSs and LBs are chosen for comparison, and the comparison result shows good agreement between PSs and LBs. The mean and standard deviation of errors (i.e. the difference between PSs and LBs) are respectively -2.02mm/yr and 3.44mm/yr. 85.22 % absolute value of errors are centralized in the range of 6mm, and the number and percentage of errors decrease with the increase of errors, as shown in figure.10.

5. STUN TECHNIQUE

In the processing system of STUN technique, the PSs are initially identified with sublook correlation method (Lijun Lu et al., 2008) instead of amplitude dispersion threshold method in the primitive STUN as it can identify PSs with a limited number of observations or even without temporal baseline. The PSs identification method is applicable for small dataset. STUN is based on the refined differential interferometric model (functional model and stochastic model). The functional model is established similar to interferometric phase model at identified PSs. And the stochastic model is also introduced to adjust the different weight for interferometric data, which contains disturbing phase terms (e.g. atmospheric artifacts and noises). On the basis of functional and stochastic model, weighted integer least-square estimator is utilized to estimate the integer ambiguity with the highest probability and the unknown key parameters including DEM error and subsidence velocity.

5.1 Processing Result

We processed the 9 latest scenes of ASAR SLC images. 83,044 PSs are identified in the test area of about 1,000km², i.e. with a density of 83 points/ km². The density of PSs in short time series is much bigger than ones in long time series as more points exhibiting phase stability in the shorter time span are identified as PSs. The subsidence velocities on the PSs from 2003 to 2005 are derived to produce the subsidence map, as showed in figure.6.

5.2 Validation

In the test area, 177 LBs ranked Level 1 and Level 2 are measured from 2003 to 2005 year, as showed in figure.7. There are two levelling campaign in this period. The average of two surveys is used as the criterion to validate the result in short time series.

Nearest neighboring method is also used to validate PSs computed by STUN. As shown in figure.9, there are 140 pairs of PSs and LBs chosen for comparison, and the result shows good agreement between PSs and LBs. However, we also notice that a few bigger errors appear and the possible cause may be that subsidence variation does not fit the referred the linear model. The mean and standard deviation of errors are -2.01mm/yr and 4.30mm/yr respectively. Seen from figure.11, 79.29% absolute value of errors are centralized in the range of 6mm, and the number and percentage of errors decrease with the increase of errors.

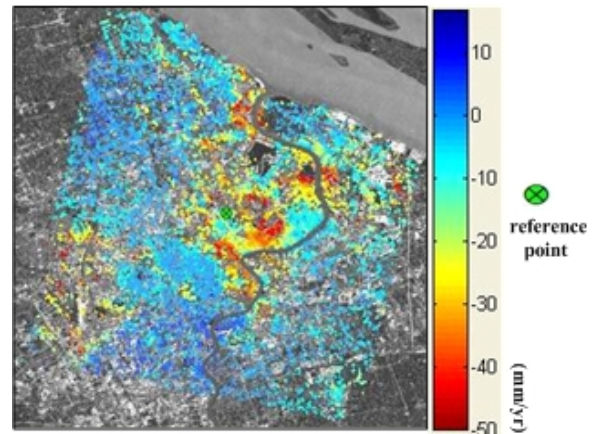


Figure 4. Subsidence velocity map in 1993-2000

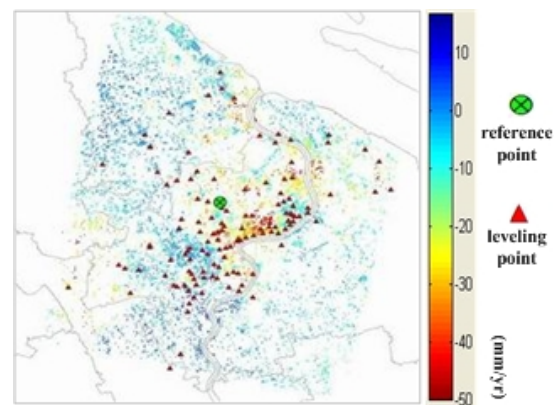


Figure 5. The Levelling Benchmarks surveyed in 1993-2000

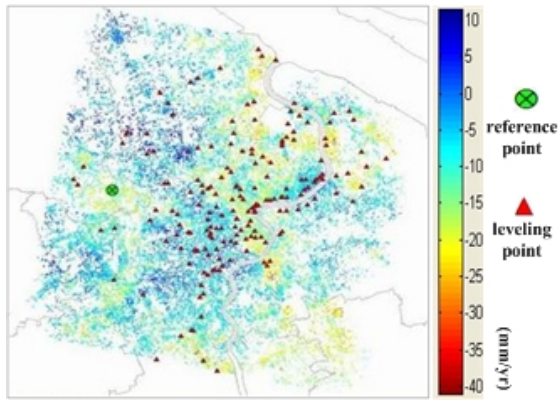


Figure 6. Subsidence velocity map in 2003-2005

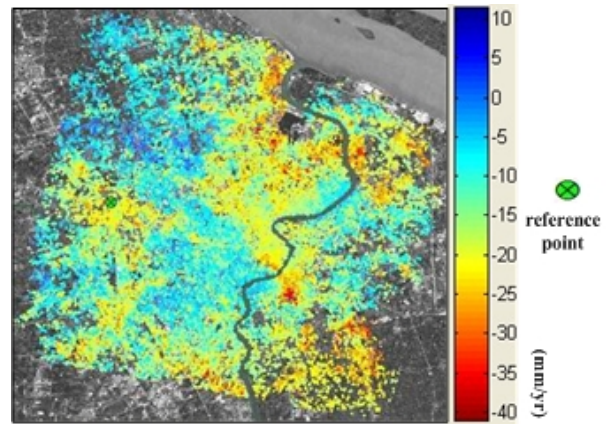


Figure 7. The Leveling Benchmarks surveyed in 2003-2005

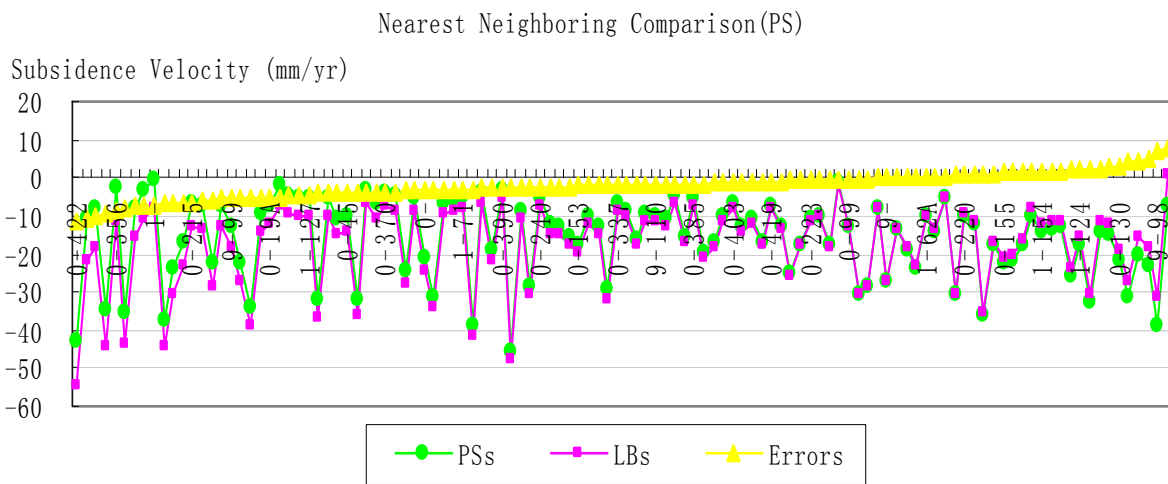


Figure 8. The comparison between LBs and PSs by nearest neighboring method to validate the PS technique

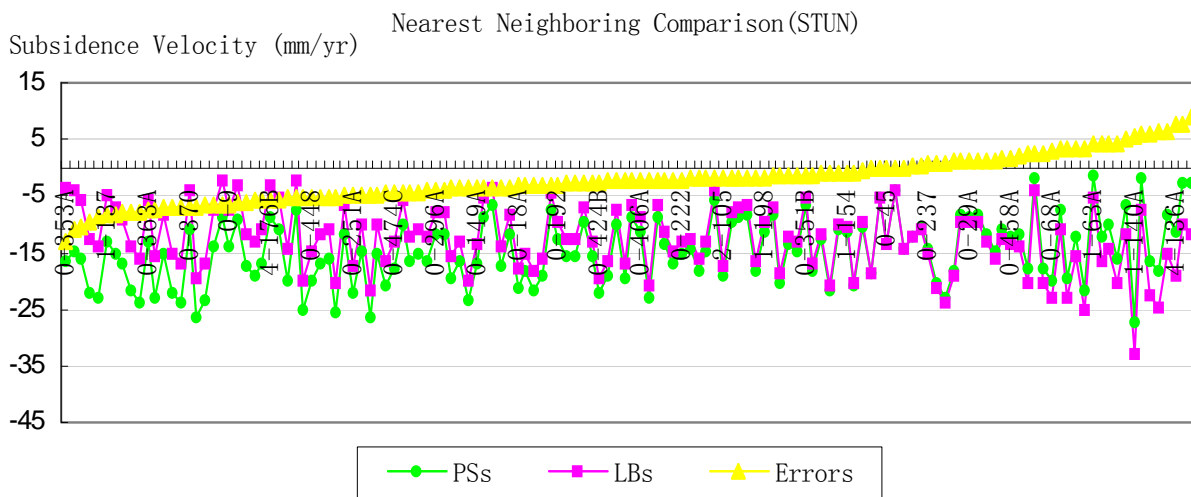


Figure 9. The comparison between LBs and PSs by nearest neighboring method to validate the STUN technique

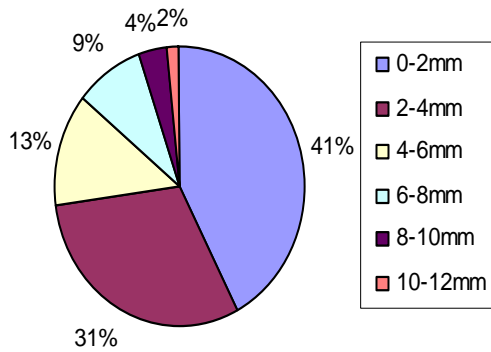


Figure 10. The percentage of errors by PS technique

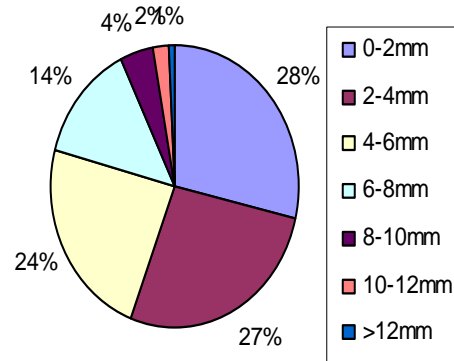


Figure 11. The percentage of errors by STUN technique

6. DISCUSSION AND ANALYSIS

From the subsidence results shown in the figure 4 and figure 6 of two periods, we can find the distribution of main subsidence regions are basically uniform. In order to probe into the cause and change of subsidence in recent years in Shanghai urban, we divide the test area into 5 regions according to the districts of Shanghai. We can analyze the cause in the following two aspects: exploitation of underground water showed in figure. 13 (we use pumpage of ground water in 2000 as the average pumpage since annual pumpage of ground water remains almost unchanged in the past decade) and urban land use showed in figure. 14 (including the use of residence land, industrial land, commercial land and municipal engineering constructions in 2005). And we also can describe the change of the subsidence in test area according to the above processing results in two different periods.

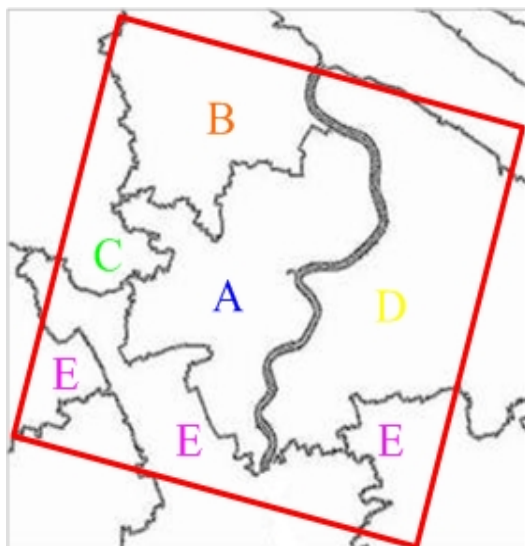


Figure 12. A-E regions in test area

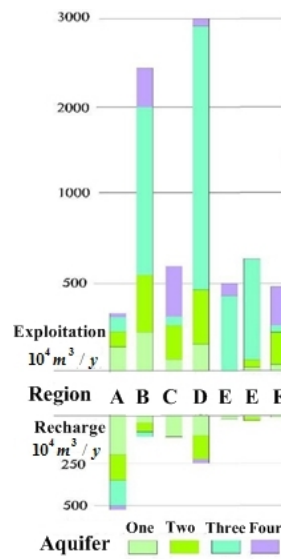


Figure 13. The pumpage of ground water of 5 regions of Shanghai in 2000

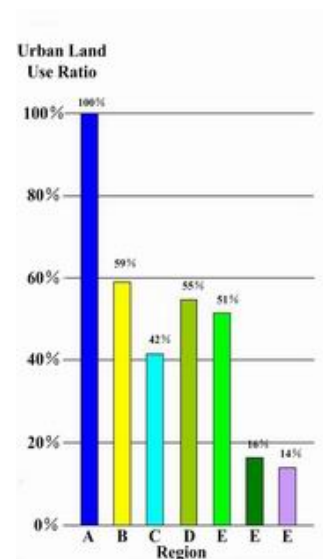


Figure 14. The urban land use ratio of 5 regions of Shanghai in 2005

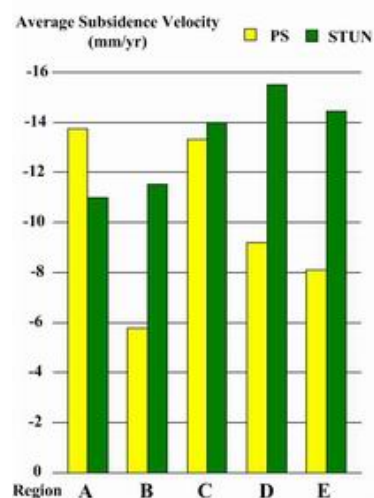


Figure 15. Comparison of average subsidence velocities obtained by PS in 1993-2000 and that by STUN in 2003-2005

A — it represents the centre urban of Shanghai where the severe subsidence has occurred. As shown in figure.13, the pumpage of ground water is smaller than 5 million m³/ yr, and the recharge of a large amount of ground water is undertaken to control subsidence. With the rapid development of centre urban in recent years, the urban land use ratio has reach 100% (figure.14). Comparing the subsidence results of two periods (figure.15), the average subsidence velocity is slowing down. Hence we can deduce that subsidence due to exploitation of underground has been mitigated to under the control, while subsidence due to urban land use has become the predominant cause.

B — it represents one new town of Baoshan in Shanghai. Severer subsidence occurred in the East of Baoshan. As shown in figure.13, the huge pumpage of ground water is larger than 20 million m³/ yr, and as an important industrial base of metallurgy, the land use ratio of the town exceeds 50% (figure.14). Comparing the results of two periods (figure.15), the magnitude of subsidence is increasing. Hence we can deduce that exploitation of under ground water is the main cause of subsidence and tendency of subsidence is speeding up.

C — it represents a developing new town of Jiading in Shanghai. As shown in figure.13, the pumpage of ground water is approximately 5 million m³/ yr, and as a new developing town, the urban land use ratio of the town is only 40% (figure.14). The study area of C region is very small in the new town, but it takes up a large proportion of subsidence area. Average subsidence velocities in two periods are basically the same (figure.15). We can deduce that exploitation of under ground water leads to a majority of subsidence in C region.

D — it represents a high and new technology industrial development town of Pudong in Shanghai. As shown in figure.13, the huge pumpage of ground water is approximately 30 million m³/ yr, and some measures of recharge is taken to relieve the over-pumping. As the most developed industrial zone, the urban land use ratio of the town is 54% (figure.14), and the developed lands mainly consists of large plants and municipal engineering constructions. Average subsidence velocity is becoming faster (figure.15). We can deduce that exploitation of under ground is the main cause of subsidence and the land use accelerate the process.

E — it represents three agricultural towns of Minghang, Nanhui and Qingpu in Shanghai. The study area of E region includes a part of three towns. As shown in figure.13, the pumpage of ground water of each of three towns is approximately 5 million m³/ yr. Being agricultural towns, urban land use ratio of each town is not more than 51% (figure.14). Average subsidence velocity accelerates due to pumping of ground water in the new aquifer, e.g. the exploitation in the fourth aquifer in Nanhui town. We can deduce that exploitation of under ground water is the main cause of subsidence and tendency of subsidence is speeding up.

The above analysis gives us an impression that subsidence disaster in Shanghai urban is mainly caused by joint action of exploitation of ground water and urban land use. Exploitation of ground water is still the main cause leading to subsidence and the urban land use accelerates the process. The measure of recharge has been taken to control subsidence so that the subsidence of some regions has mitigated. But with the rapid development of urban area, urban land use has become a new

cause leading to subsidence and shown extending tendency in some regions.

Owing to lack of a great deal of detailed ground truth data, the quantitative analysis concerning the relations among the subsidence, pumpage of ground water and land use status has not been made in the paper, and more in-depth studies will be conducted in the future.

7. CONCLUSIONS

In this paper, the two PS-InSAR techniques are applied in long-term and short-term subsidence measurements are proved to be effective in Shanghai urban, and it suffices to meet different needs of survey tasks. On the other hand, the cause of subsidence and subsidence variation of two periods are qualitatively analyzed to provide a guidance to detect and control subsidence disaster for decision-making department.

REFERENCES

- Best M. Kampers, 2006. RADAR INTERFEROMETRY Persistent Scatterer Technique. Springer, Germany, pp.43-66.
- Ferretti, A., Prati, C., Rocca, F., 2001. Persistent scatterers in SAR interferometry. IEEE Transactions on Geoscience and Remote Sensing, 39(1), pp. 8 – 20.
- Ferretti, A., Prati, C., Rocca, F., 2000. Analysis of Permanent Scatters in SAR Interferometry. Geoscience and Remote Sensing Symposium. Proceedings[C]. IGARSS 2000, 2 pp.761-763.
- Li D R, Liao M S, Wang Y, 2004. Progress of Permanent Scatterer Interferometry. Geomatics and Information Science of Wuhan University. 29(8), pp.664-668.
- Lijun Lu, Mingsheng Liao, Changcheng Wang. etc, 2008. A New Method of Identification of Stable Pointwise Target in Small SAR Dataset. Proceedings of the 2008 Dragon Symposium - Dragon Programme Final Results Results (in press).

ACKNOWLEDGEMENTS

The work in the paper was supported by the National Key Basic Research and Development Program of China (Contract No. 2007CB714405) and 863 High Technology Program (Contract No. 2006AA12Z123). The authors thank ESA for providing the SAR data through ESA-NRSCC Cooperational Dragon Programme (id: 2567). And the author would also thank the Shanghai Institute of Geological Survey for providing the ground validation data.